ELSEVIER

Journal of Structural Geology 27 (2005) 597–606

JOURNAL OF STRUCTURAL GEOLOGY

www.elsevier.com/locate/jsg

Geometric description of flanking structures

Sara Coelho[a,*], Cees Passchier[a], Bernhard Grasemann[b]

[a]*Department of Geosciences, University of Mainz, Becherweg 21, 55099 Mainz, Germany*
[b]*Department of Geological Sciences, University of Vienna, Austria*

Received 4 August 2004; received in revised form 30 November 2004; accepted 7 December 2004
Available online 19 February 2005

Abstract

Present nomenclature of faults and flanking structures is ambiguous. This paper presents a system for description of flanking structures, based on geometric parameters and independent of kinematic frame. The description can be made using two levels of accuracy. A qualitative method is described using four geometric features: tilt, slip, lift and roll. This method is suggested for practical use in the field, since it does not involve measurements or complicated procedures. In parallel, a quantitative approach is also presented, based on analytical modelling of Bézier curves. This method requires measurement of geometric features and involves mathematical treatment, but allows comparison between different flanking structures.

Keywords: Flanking structure; Shear zone; Fault drag; Reverse drag; Fault classification

1. Introduction

Since the first applications of geology in underground mining, people have felt the need to classify geological structures such as faults according to orientation and displacement direction (e.g. Playfire, 1802). At first sight, the geometry of faults cross-cutting layering in rocks seems simple enough not to warrant further thought. Empirical data led to a simple scheme of normal faults, which were the most common in mining areas set in extensional basins, and reverse (or thrust) faults. Further detail was added by Suess (1885) and de Margerie and Heim (1888) who introduced the concept of *fault drag*, the deflection of layers in the vicinity of the fault. Later, fault drag was subdivided into *normal* and *reverse drag* by the work of Hamblin (1965).[1] In combination with the terms footwall and hanging wall, the system seems unambiguous. However, in the sedimentary basins where this fault nomenclature was mainly defined, fault drag usually involves little deflection of layering or foliation towards the faults. In metamorphic, highly deformed rocks, or in more complex systems of faults, geometries produced by fault drag can be more complex. A simple example can describe the kind of ambiguity that can arise in certain cases. The structure depicted in Fig. 1 is an example of a complex structure that deserves careful description in order to avoid misinterpretations. It can be originated in one single deformation episode (cf. Exner et al., 2004) and a natural example is shown in Fig. 8a. The structure can be described both as a normal fault or a thrust in the existing classification. An observer on the scale of the smaller box observes a displacement in the marker typical of normal faults. If the structure is observed only in the far-field (bigger box) one might interpret it as a thrust. This example shows the need of describing accurately the fabric of fault drag, combined with the far-field displacement, in order to make correct interpretations.

Passchier (2001) and Grasemann and Stüwe (2001) expanded the concept of fault drag and defined *flanking structures* also known as *flanking folds*, developed where a host element (HE) is deflected in the vicinity of a cross-cutting element (CE) (Fig. 2). The host element is a planar feature in the fabric of the rock, such as bedding, metamorphic foliation or compositional layering. The

* Corresponding author
E-mail address: sarasscoelho@yahoo.co.uk (S. Coelho).

[1] Note that the widespread concept of *drag folds*, as defined by Leith (1914) and researched by Ramberg (1963) describes subsidiary folds, parasitic folds or minor folds produced by differential movement of adjacent layers.

0191-8141/$ - see front matter © 2005 Elsevier Ltd. All rights reserved.
doi:10.1016/j.jsg.2004.12.002

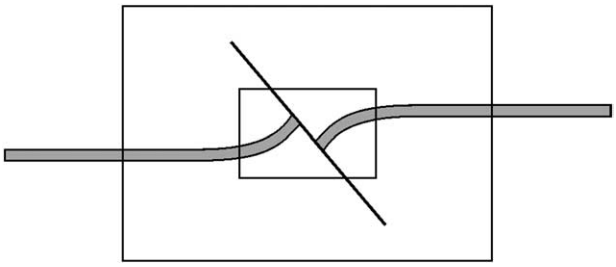

Fig. 1. Example of the ambiguity of fault nomenclature. Considering the arrangement of layering (bigger box) the structure may be classified as a thrust. However, based on displacement close to the fault (small box) the structure would be interpreted as a normal fault.

cross-cutting element is the central part of the flanking structure and can be a fault, a joint, a filled vein, a patch of melt or even a rigid object in the rock such as a mineral or a boudin (Passchier, 2001). Flanking structures were initially envisaged as sub-metre scale structures, but geometrically they can include features such as fault drag, fault bend folds, and any fold developed around an object in a matrix, such as metadolerite dykes (Gayer et al., 1978) and crevasses in ice (Hudleston, 1989). The concept can also include folds developed due to rotation of a rigid object in a matrix, such as the drag folds modelled and described analytically by Ghosh (1975).

Grasemann and Stüwe (2001) and Grasemann et al. (2003) investigated the development of flanking structures adjacent to a cross-cutting element, by simulation of flow around a slip surface in a viscous medium under general shear, by means of finite element modelling. Part of this work was a first attempt to classify flanking structures into three main categories: a-, s- and n-type flanking structures, which can be subdivided into 11 sub-types named A–K (cf. Passchier, 2001; Grasemann et al., 2003). Although this genetic classification, which presumes a known kinematic frame, has been used in forward modelling studies (Exner et al., 2004; Wiesmayr and Grasemann, 2004), field studies have shown that this classification is imprecise and ambiguous when describing natural flanking folds.

In this paper we propose a non-genetic uniform classification system for all types of flanking structures, based solely on geometric criteria in order to avoid up-stream interpretation errors. This can be done with two levels of accuracy. A qualitative method is proposed as a descriptive tool to use in the field, while a quantitative method, based on analytical modelling, is also introduced where greater accuracy is needed, such as for comparison of flanking structures. With this method, the classification of flanking structures based on a-, s- and n-types and their 11 sub-types A–K becomes obsolete.

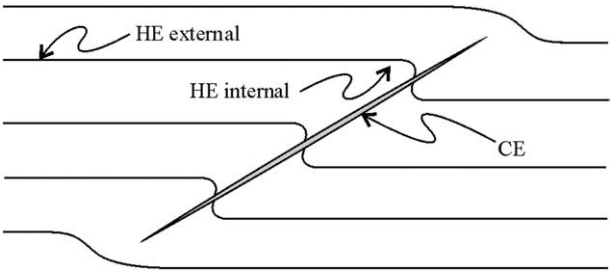

Fig. 2. Schematic representation of a flanking structure. HE—host element, the external far-field component is unaffected by the flanking structure; the internal part of the host element is folded and defines the flanking structure. CE—cross-cutting element.

2. Qualitative classification

The geometry of faults, objects or veins and associated flanking structures can be described by a HE and a CE (Fig. 2). The HE can be subdivided into an external unfolded part, parallel on both sides of the CE (far-field component), and an internal part where the HE can be folded in a complex way. Here we restrict ourselves to simple fold geometries, which are enough to fully describe and classify most flanking structures.

A flanking structure, on one side of the CE, can be described using four parameters, defined according to the geometric relations between the HE and the CE, in a fixed reference frame (Fig. 3). The origin of a Cartesian coordinate system is set at the intersection of the CE and HE. The *x-axis* is oriented to be parallel with the far-field HE, with its positive half according to the dip of CE. In the following text, only hanging wall positions above the CE are described, although the method equally applies to flanking structures in the footwall. In strike slip, this corresponds to the wall away from the observer. This means that the positive *y-axis* is always in the same block as the positive *x*-axis. Notice that by defining the origin in the HE–CE intersection, only the geometry of one side of the CE is described, and that two separate coordinate systems have to be drawn for each side of the CE. This may seem an unnecessary complication but is useful, since flanking structures in the same layer commonly have a different shape on both sides of the CE.

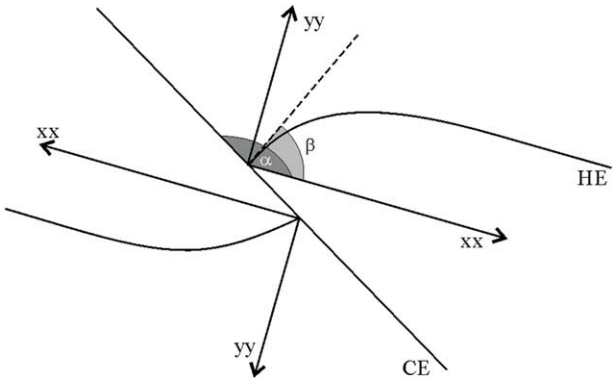

Fig. 3. Geometric features of an idealised flanking structure. HE—host element; CE—cross-cutting element; α—angle between CE and the *x*-axis; β—angle between the tangent to HE at the intersection with CE and the *x*-axis.

The four different parameters describing a flanking structure are defined according to the geometric relation between the host element HE and the cross-cutting element CE in a cross-section through the structure, such as shown in Fig. 2. Ideally this is the section normal to the intersection of CE and HE. These parameters are *tilt*, *slip*, *lift* and *roll*, illustrated in Figs. 4 and 5.

Tilt (angle α) is defined as the trace of dip of the CE (Fig. 4a). The Cartesian coordinate axes are drawn to represent a positive *x*-axis in the sense of the dip. Due to this geometry, tilt is given by an angular value α, measured between the *x*-axis and the CE, ranging between 90 and 180° (Fig. 3). This convention is advantageous because it does not allow double geometries of mirror-image structures.

Slip is the displacement (off-set) of the HE observed on the CE surface (Fig. 4b). Slip is also a completely independent parameter, since its value does not depend on the geometry of the flanking structure itself, but on the relationship with the other half of the structure. This is fortunate for description purposes because sometimes the absence of clear markers make it difficult to observe slip in the field. As an independent parameter, slip can be conventionally defined as being positive if against the sense of dip of the CE (tilt), negative if according to dip and neutral if inexistent. When other independent shear criteria are present, slip description can be refined using the nomenclature of Grasemann and Stüwe (2001): *co-shear slip* if in the same sense of the regional shear sense and *counter-shear slip* if opposite.

Lift is the far field displacement of the external HE measured with respect to the *x*-axis (Fig. 4c). It is a parameter independent of tilt and slip. Lift is considered positive when the HE is above the *x*-axis and negative in the opposite situation. Notice that this definition only includes one side of the flanking structure. This is useful because correlation between layers on both sides of the CE is sometimes difficult. Moreover, it allows definition of lift when a counterpart is absent, such as in the case of flanking

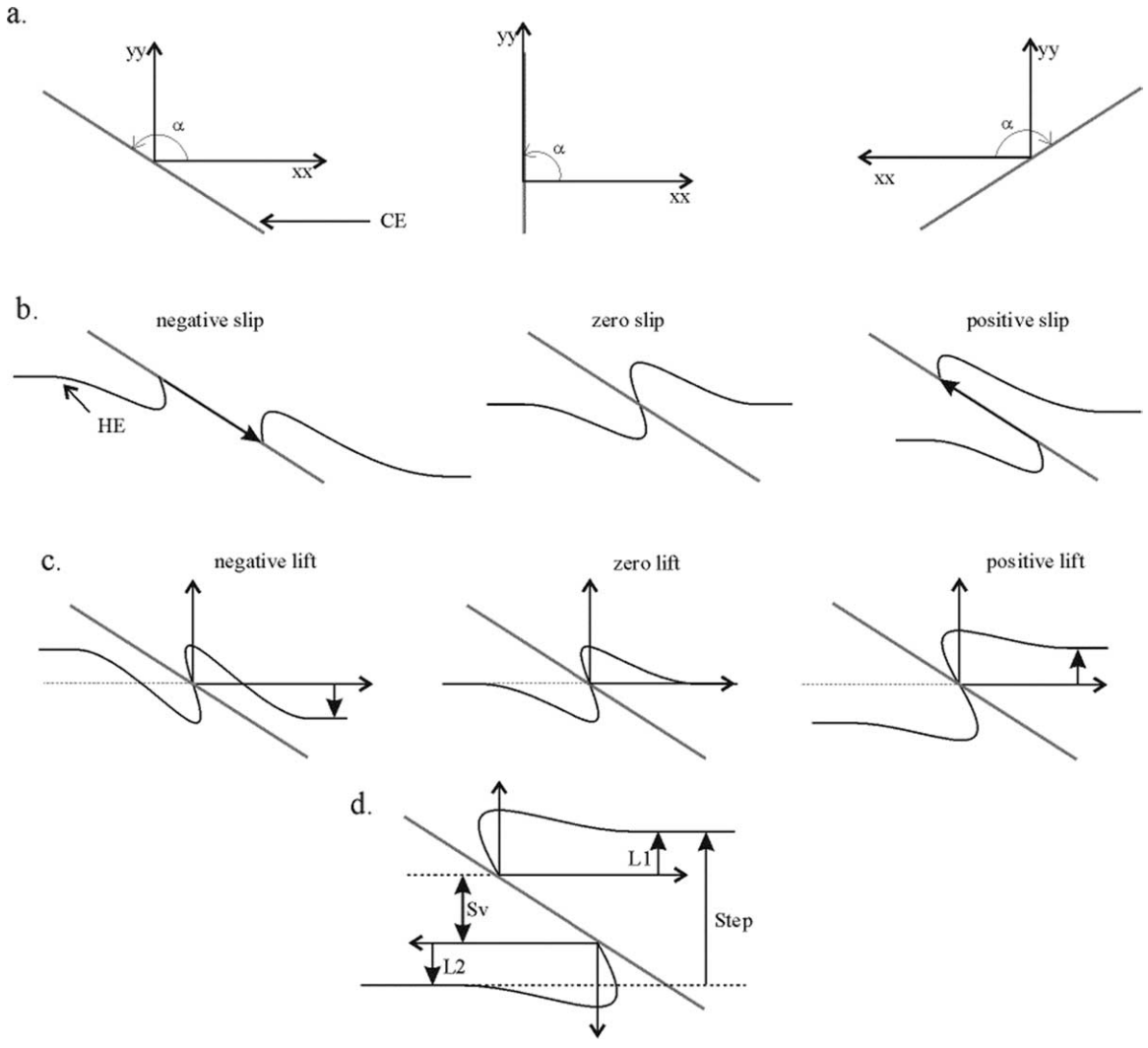

Fig. 4. Schematic diagram showing the nature of variation of the three parameters that define the geometry of flanking structures. (a) Tilt—dip of the CE and the resulting orientation of the coordinate axis system; (b) slip—offset of the HE along the CE surface, shown by arrows; (c) lift—elevation of the HE above or below the *x*-axis; (d) definition of step as the sum of L1 and L2 (two lifts) and Sv, the vertical component of slip. CE and HE as in previous figures.

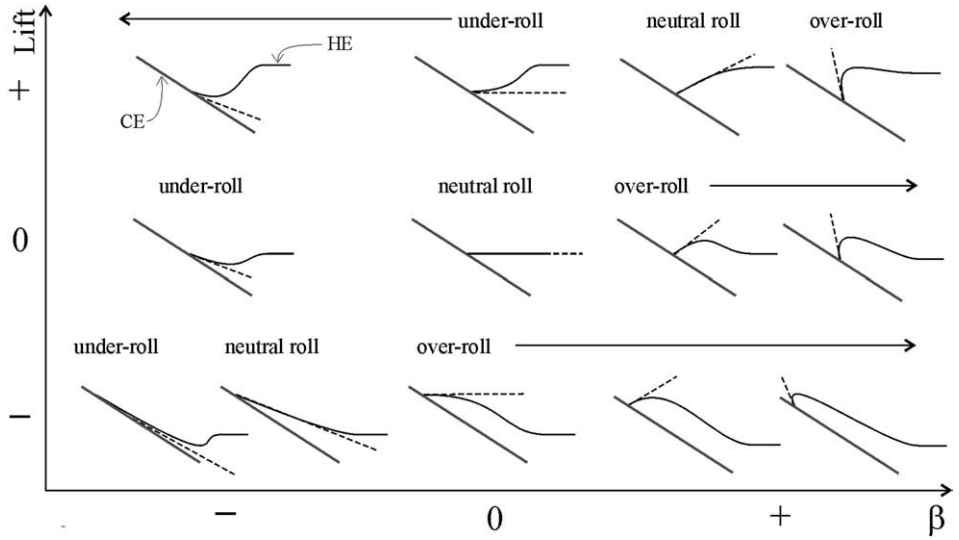

Fig. 5. Schematic representation of roll, according to lift and β-angle values. Tilt is constant throughout the figure. β-angle is measured between the tangent of HE at the intersection with CE (dashed line) and the x-axis. Neutral roll: single curvature; under- and over-roll: double curvature facing up or down, respectively. Notice that the position of neutral roll varies with lift, showing the dependence of roll on this parameter. CE and HE as in previous figures.

structures around rigid objects. If a correlation of layers can be established across the CE, we can define a parameter *step* as the orthogonal distance between the HE of the hanging wall and footwall in the far field. This means that, if the layering is horizontal, step is equal to *throw*, a term that is frequently used in petroleum geology (Fig. 4d). Step is the sum of the lift of corresponding parts of a HE on both sides of a CE, plus the vertical component of slip. This parameter, although useful for description purposes of symmetric flanking structures, will not be used in the following classification.

Lift, slip and tilt cannot describe the geometry of flanking structures completely since the shape of the curve that connects the straight, far field part of HE with the cut-off point on the CE can vary considerably (Fig. 5). *Roll* describes the magnitude and sense of this curvature (Fig. 5), as follows. Roll is best thought of in terms of the direction of curvature when moving along the HE from the far field towards the cut-off point. If this is a smooth fold with a single direction of curvature, roll is neutral; neutral roll is an open flanking fold structure with two limbs. In the special case where lift is zero and roll is neutral, the flanking structure is a straight layer that ends at the CE. Neutral roll flanking structures can be enhanced with *bulge* (Fig. 6), without loosing their single curvature characteristic feature. A flanking fold with bulge has a stronger curvature than an envisaged minimum value as shown in Fig. 6.

If there is a change in the direction of curvature from the far field HE to the cut-off point, roll is not neutral, and the flanking fold has three limbs. In other words, curvature is composite and has an inflexion point. In the reference system as shown in Fig. 5, if the curvature faces down, the flanking structure has over-roll; if the curvature faces up, the flanking structure has under-roll (Fig. 5). Due to the nature of double curvatures, all under- and over-roll flanking structures have bulge by default.

Roll differs from the other parameters in that it is heavily dependent on *lift*, although independent of slip and tilt. Nevertheless, as shown in Figs. 5 and 6, it cannot be described in terms of lift only.

The angle β, measured between the x-axis and the tangent of the flanking structure at the intersection with the CE (Fig. 3), can be useful to refine the geometric description. Keeping lift constant, a variation of the angle β from negative to positive values, produces an evolution of roll, from under-roll to over-roll structures (Fig. 5). Note that in this instance, the neutral roll case does not necessarily correspond to $\beta = 0$. In neutral roll flanking structures, β is mainly responsible for the presence or absence of bulge (cf. Fig. 6). This angle ranges, in theory, between $-180°$ and $180°$, but in practise is limited by the amount of tilt, since a realistic flanking structure never crosses its own cross-cutting element ($\beta < \alpha$).

Excluding tilt, which is not directly related to the geometry of the flanking structure itself, the combinations

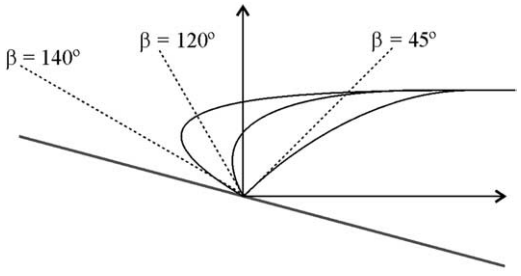

Fig. 6. Three examples of flanking structures with neutral roll (that is, flanking structure without an inflexion point) and variable bulge. At $\beta = 45°$, the flanking structure has minimal bulge; with increasing β the bulge becomes more enhanced.

of slip, lift and roll define a set of 27 theoretically possible geometries (Fig. 7).

2.1. Example

Fig. 8a gives an example of a flanking structure developed in marbles from Naxos Island (Greece) around a quartz vein. Drawing the appropriate coordinate systems (Fig. 8a, box) and using the parameters outlined above, the flanking structure can be described as: lift positive; slip negative and neutral roll with bulge. This classification applies to both sides of the flanking structure (I and II), despite the fact that in this natural example they are not absolutely equal in shape: the curve in I has a more enhanced bulge than II, although they are both neutral roll examples. In practice there can be gradients in the parameters from layer to layer along a CE.

Fig. 8b is an example of flanking structures around a quartz vein in marbles, this one from a marble unit in Namibia. The flanking structure in the central layer is described as lift negative, slip positive and neutral-roll. In this example, shear sense is sinistral according to independent criteria (not shown in the picture) and thus slip may be further classified as counter-shear slip.

Qualitative description of flanking structures is suggested for use as a field tool, since it is based on parameters that are easy to recognize and does not involve measurements or a detailed analysis. However, this qualitative description does not allow an accurate comparison between outcrops, or even flanking structures within a single occurrence. The quantitative description outlined below is based on analytical modelling of Bézier curves and quantifiable parameters and is more adequate for detailed studies.

3. Quantitative description

The use of Bézier curves as a tool to describe curvatures and surfaces was introduced by French engineers of the automobile industry, in particular Bézier (1966, 1967). More recently, the concept was recognised as useful in geological description (De Paor, 1996) and used as a tool for fold shape analysis (Srivastava and Lisle, 2004). In this paper we apply the concept to flanking structures.

A general cubic Bézier curve (Fig. 9a) is described by the Cartesian coordinates of a set of four node-points *a*, *b*, *c*, and *d*. Each point on the curve is given as a function of these

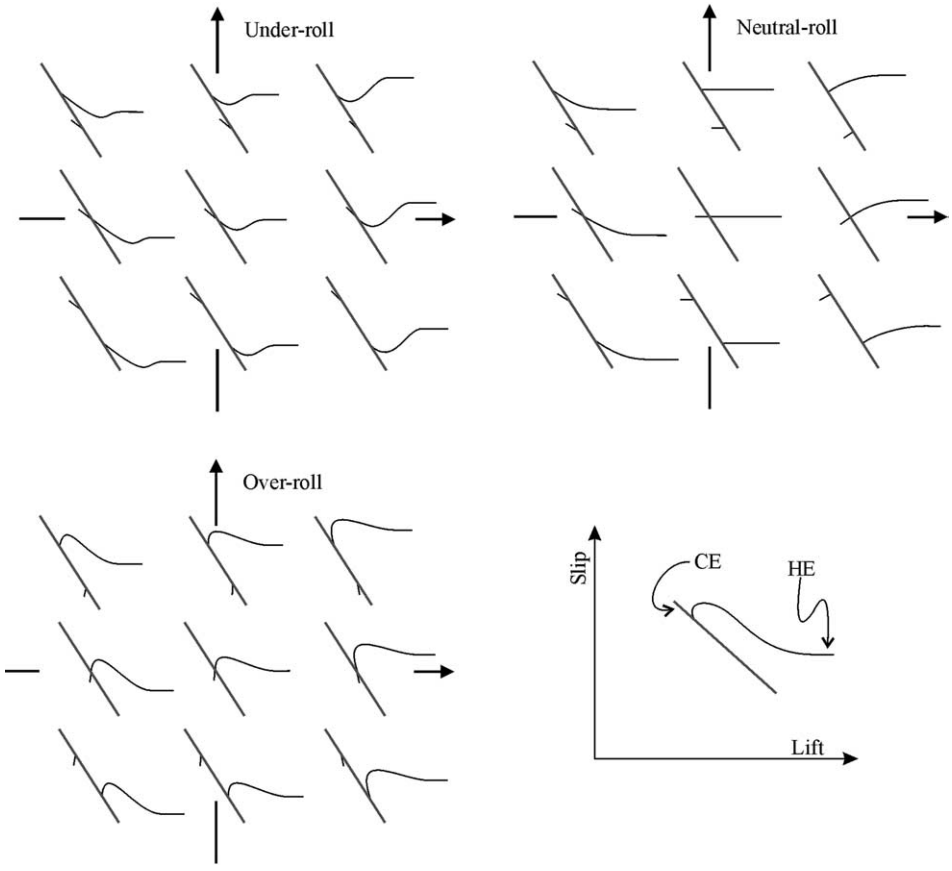

Fig. 7. The 27 theoretical geometries of flanking structures, classified according to lift, slip and roll parameters. Notice that variations in tilt (orientation of the CE) can add additional possibilities but do not affect the basic geometry of the structures. CE and HE as in previous figures. Only one side of the flanking structures is represented in full, since each side can have a different geometry.

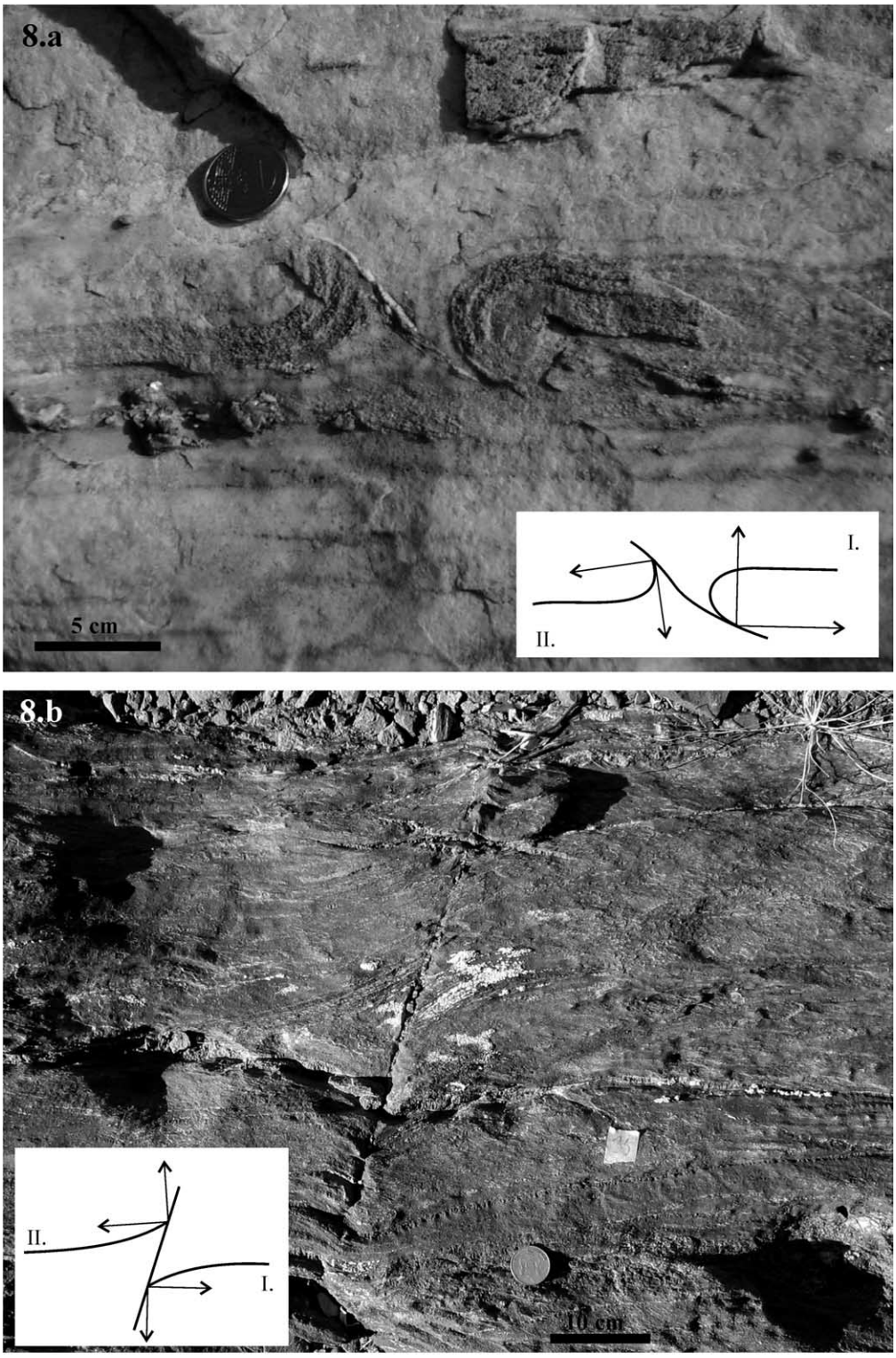

Fig. 8. Field examples of qualitative description of flanking structures. (a) Example from marbles on the Island of Naxos (Greece)—slip negative; lift positive and neutral roll with bulge; (b) example from the "House of the German" limestone (Namibia)—slip positive, lift negative and neutral-roll. See text for discussion.

node points and of t, a spatial parameter variable between 0 and 1. The two governing parametric equations are an expansion of Bernoulli polynomials and, for the case of a cubic Bézier curve, they can be written as:

$$x(t) = (1-t)^3 x_a + 3(1-t)^2 t x_b + 3(1-t)t^2 x_c + t^3 x_d$$

$$y(t) = (1-t)^3 y_a + 3(1-t)^2 t y_b + 3(1-t)t^2 y_c + t^3 y_d \quad (1)$$

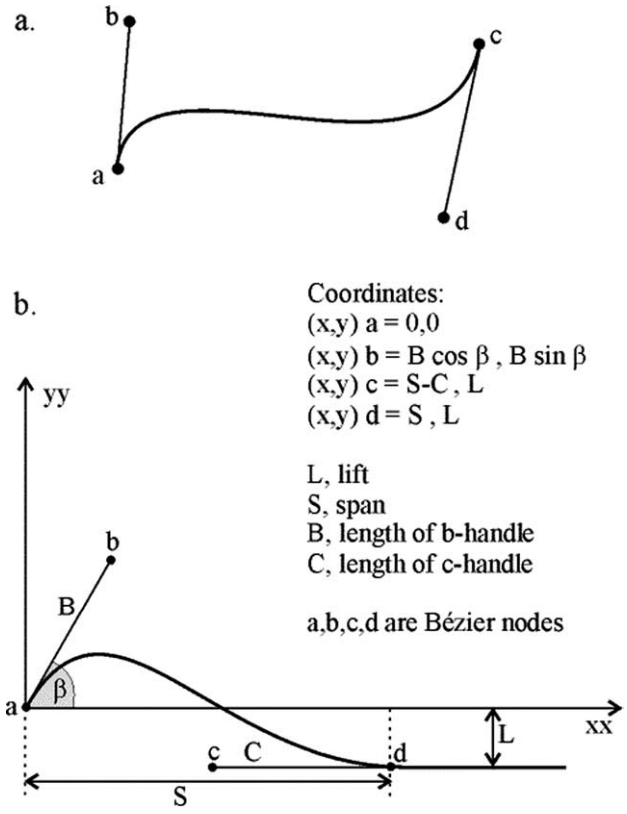

Fig. 9. (a) General cubic Bézier curve, with node points *a*, *b*, *c* and *d*. (b) Cubic Bézier curve, adapted to the concept of flanking structures. See text for discussion.

The equation can be adapted to flanking structure geometry (Fig. 9b) because these can be described as curves, as De Paor (1996) and Srivastava and Lisle (2004) already demonstrated for folds. However, some adaptations are required. Node-point *a* can be defined as the HE–CE intersection and *d* as the first deflection of the host-element attributed to the flanking structure effect. *b* and *c* are Bézier nodes with no geological equivalent. Thus, *a* is the origin of the coordinate system, x_d is always positive and $y_c = y_d$. The later assumption prevents curves with sharp bends where a flanking structure grades into the far-field layer geometry. Although such sharp bends are possible as abstract geometries, they are geologically unrealistic.

With these assumptions the general parametric Eq. (1) can be rewritten as:

$$x(t) = (3x_b)t + (-6x_b + 3x_c)t^2 + (3x_b - 3x_c + x_d)t^3$$

$$y(t) = (3y_b)t + (-6y_b + 3y_d)t^2 + (3y_b - 2y_d)t^3 \quad (2)$$

Some of these parameters can be determined by detailed field analysis of the flanking structures (Fig. 9b). y_d is the mathematical equivalent of the *Lift* (*L*) parameter discussed previously in this work. x_d can be defined as the *Span* (*S*) of the flanking structure. x_b and y_b can be described as polar coordinates using angle β (which can be directly measured from field examples) and *B*, the length of the Bézier handle *b*.

After the appropriate substitutions and simplifications, Eq. (2) becomes:

$$x(t) = (3B\cos\beta)t + (-6B\cos\beta + 3S - 3C)t^2 + (3B\cos\beta - 2S + 3C)t^3$$

$$y(t) = (3B\sin\beta)t + (-6B\sin\beta + 3L)t^2 + (3B\sin\beta - 2L)t^3 \quad (3)$$

In order to allow comparison between studied examples, it is useful to normalize these equations and transform its parameters into dimensionless numbers. The chosen normalization parameter is the Span, *S*. Eq. (3) can thus be rewritten as:

$$\begin{cases} \bar{x}(t) = (3\bar{B}\cos\beta)t + (-6\bar{B}\cos\beta + 3 - 3\bar{C})t^2 + (3\bar{B}\cos\beta - 2 + 3\bar{C})t^3 \\ \bar{y}(t) = (3\bar{B}\sin\beta)t + (-6\bar{B}\sin\beta + 3\bar{L})t^2 + (3\bar{B}\sin\beta - 2\bar{L})t^3 \end{cases} \quad (4)$$

where $\bar{x} = x/S$; $\bar{y} = y/S$; $\bar{B} = B/S$; $\bar{C} = C/S$; $\bar{L} = L/S$.

If the shape of a natural flanking structure is fitted to a Bézier curve defined by Eq. (4), dimensionless numbers $\bar{B}$, $\bar{C}$, $\bar{L}$ and β can be derived to characterize its shape. The parameters β, *S* and $\bar{L}$ can be obtained from field examples. $\bar{B}$and $\bar{C}$, the lengths of the Bézier-handles (Fig. 9b), can be estimated using a simple spreadsheet and a graphic in conjunction with Eq. (4). In a Bézier curve, these two handles determine the shape of the geometric curve and it is important to understand their behaviour before attempting an estimation of parameters.

The length of the normalised *B*-handle controls, with respect to the coordinate system, the vertical shape of the flanking structure (Fig. 10). Relatively big $\bar{B}$ values are associated with over- or under-roll. On the other hand, the normalised *C*-handle is responsible for the horizontal extension of the structure, again with respect to the coordinate axis. Large $\bar{C}$ values will make the curvature sharper, whilst open gentle curves are expected when $\bar{C}$ is low.

The analytical modelling presented above considers cubic Bézier curves, based on third degree Bernstein polynomials. It is possible to increase accuracy in the definition of the flanking structures by increasing the degree of the Bézier curve itself. This procedure, however, leads to equations of the fourth or fifth degree. We felt that the extra detail accomplished does not warrant the unpractical increasing complexity of classification.

3.1. Example

To illustrate the usefulness of the quantitative method here presented, we chose a set of flanking structures developed around a fault in a marble unit in Namibia (Fig. 11a). Here flanking structures are highly variable in shape from layer to layer along the CE (Table 1; qualitative description line), although parameter slip is positive along

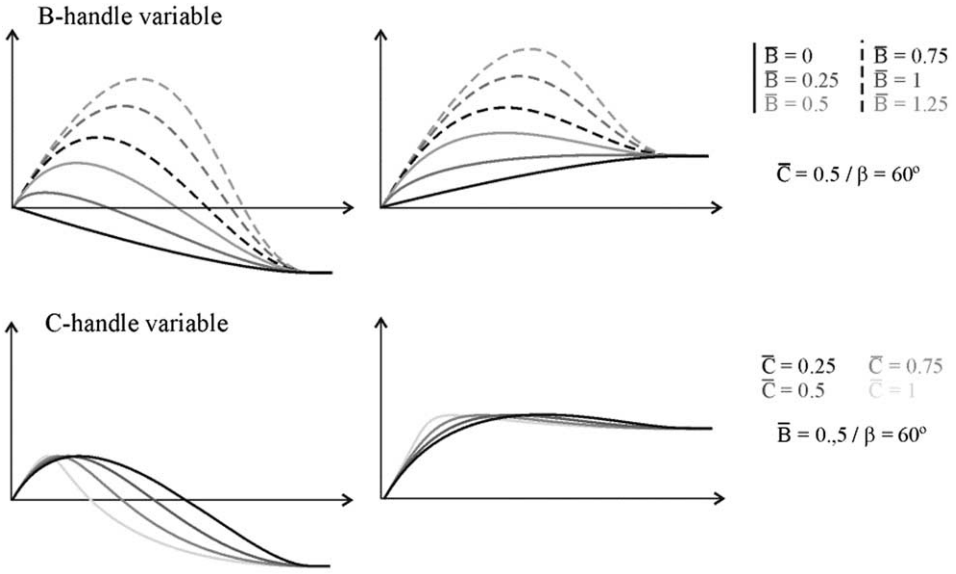

Fig. 10. Effect of length of the *B*- and *C*-handles on the shape of the flanking structures.

the entire fault. The first step to compare the flanking structures in different layers is to sketch the whole structure. Then, the parameters *S*, *L* and angle β are measured in all selected points (Table 1). Since the equations consider normalized non-dimensional parameters, the measuring unit is not relevant. Also, due to the normalization of the span, it is possible and more practical to choose a common span value for all structures since, in most natural examples, it is difficult to determine with precision the first inflexion of the flanking structure (Fig. 9b). Using a spreadsheet program and Eq. (4), parameters $\bar{B}$ and $\bar{C}$ can be estimated through the construction of a best fit graphic (Fig. 11c). To test the validity of this estimation, we measured the actual length of the *B* and *C* handles for each flanking structure, using the Bézier function of a drawing program. The estimated parameters, as well as the read values, are listed in the table of Fig. 11. Despite some local differences, the values show that the estimated $\bar{B}$ and $\bar{C}$ values are very close to the actual values (Table 1). Moreover, applying the correct values to Eq. (4) returns a graphic very similar to that obtained with estimated parameters. Although we understand that estimation introduces error, we are confident that this error will have only a minor implication in the overall results.

The quantitative parameters $\bar{B}$ and $\bar{C}$, both estimated and exact, as well as $\bar{B}$ and $\bar{L}$ were projected in the graphic shown on Fig. 11d. This allows visualization of the gradient of the referred parameters across layers along the fault. In this particular example, the quantifying method permits the following conclusions:

(1) Lift steadily decreases from the top to the bottom of the structure;
(2) *B* (Fig. 9b) remains fairly constant throughout the set;
(3) *C* is variable and, together with lift and angle β, is mainly responsible for the variable geometries observed;
(4) The flanking structures, although geometrically different, reflect a consistent evolution of parameters along the cross-cutting element.

Table 1
Quantitative parameters of the set of flanking structures shown in Fig. 11a and drawn in Fig. 11b. $\bar{L}$, normalized lift; $\bar{B}$ and $\bar{C}$, normalized length of handles *B* and *C*; estim, estimated with parametric equations; read, real value of the normalized length of handles *B* and *C*; L+/L−, positive/negative lift; Nroll, neutral roll; Oroll, over-roll; +b, with bulge

Parameters	Point 1	Point 2	Point 3	Point 4	Point 5	Point 6
Beta	85°	81°	−13°	−29°	−32°	−31°
L	0.14	0.02	−0.10	−0.29	−0.29	−0.32
$\bar{B}$ (estim.)	0.21	0.19	0.22	0.16	0.20	0.16
$\bar{C}$ (estim.)	0.26	0.73	0.67	0.61	0.64	0.63
$\bar{B}$ (read)	0.21	0.20	0.13	0.14	0.14	0.14
$\bar{C}$ (read)	0.53	0.79	0.72	0.39	0.62	0.57
Qualitative description	L+ Nroll	L+ Oroll	L− Nroll	L− Nroll	L− Nroll+b	L− Nroll−b

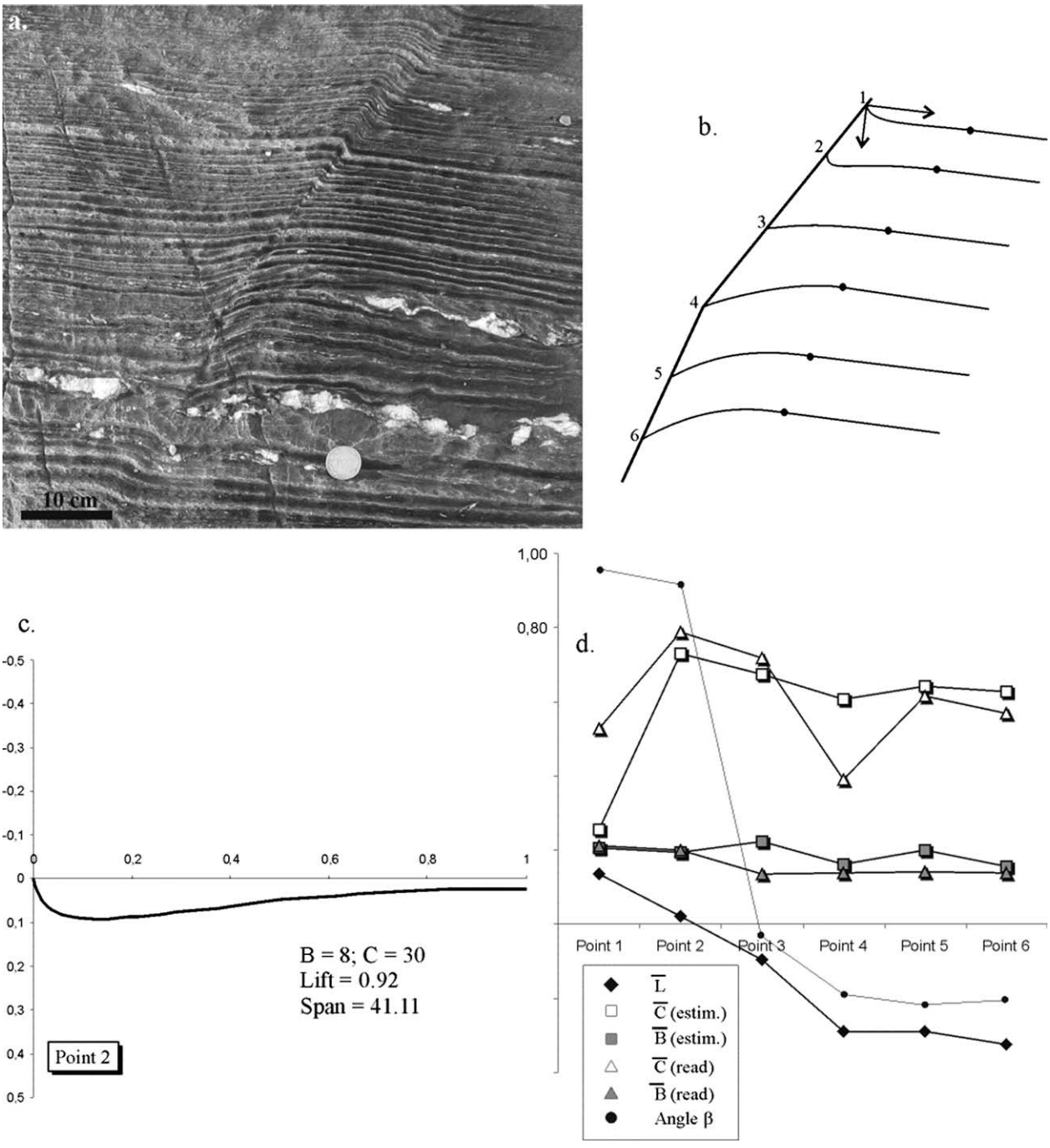

Fig. 11. Example of quantitative description of flanking structures. (a) Natural example of a set of flanking structures in limestones. (b) Sketch of the flanking structures developed around the fault. (c) Example graphic for point 2, obtained using the listed parameters and Eq. (4), discussed in text (notice that *y*-axis is inverted). (d) Graphic of the parameters, showing their evolution along the flanking structure; angle β is not to scale. See text for further discussion.

4. Conclusions

Present nomenclature of faults and flanking structures is ambiguous. We present a method that allows accurate description of flanking structure geometries observed in nature using a relatively simple set of parameters. This can be done with two levels of accuracy. A qualitative method uses the geometric features *tilt*, *lift*, *slip* and *roll*, which result in 27 different theoretical combinations that reflect virtually all possible cases observable in nature. This qualitative approach is recommended for use in field description of isolated flanking structures. A quantitative method, based on analytical modelling of Bézier curves, requires measurement of geometric features and mathematical treatment, but allows quantitative comparison between flanking structures.

Acknowledgements

SC acknowledges a scholarship from Fundação para a Ciência e Tecnologia, Portugal (FCT—SFRH/BD/12221/2003). CWP acknowledges support from DFG grant no. 2220681. BG acknowledges support from the Austrian Science Foundation (FWF grant P-15668-GEO). Comments by Yadong Zheng and an anonymous reviewer were appreciated. SC and CWP give big thanks with a smile to Rudolph Trouw and his family for friendship and hospitality. The Schürmann Foundation is thanked for financial support in Namibia.

References

Bézier, P., 1966. Definition numérique des corbes et surfaces—I. Automatisme 11, 625–632.

Bézier, P., 1967. Definition numérique des corbes et surfaces—II. Automatisme 12, 17–21.

De Paor, D.G., 1996. Bézier curves and geological design, in: De Paor, D.G. (Ed.), Structural Geology and Personal Computers. Pergamon Press, pp. 389–417.

Exner, U., Mancktelow, N.S., Grasemann, B., 2004. Progressive development of s-type flanking folds in simple shear. Journal of Structural Geology 26 (12), 2191–2201.

Gayer, R.A., Powell, D.B., Rhodes, S., 1978. Deformation against metadolerite dykes in the Caledonides of Finnmark, Norway. Tectonophysics 46, 99–115.

Ghosh, S.K., 1975. Distortion of planar structures around rigid spherical bodies. Tectonophysics 28, 185–208.

Grasemann, B., Stüwe, K., 2001. The development of flanking folds during simple shear and their use as kinematic indicators. Journal of Structural Geology 23, 714–724.

Grasemann, B., Stüwe, K., Vannay, J.C., 2003. Sense and non-sense of shear in flanking structures. Journal of Structural Geology 25, 19–34.

Hamblin, W.K., 1965. Origin of "reverse drag" on the down-thrown side of normal faults. Geological Society of America Bulletin 76, 1145–1164.

Hudleston, P.J., 1989. The association of folds and veins in shear zones. Journal of Structural Geology 11, 949–957.

Leith, C.K., 1914. Structural Geology. Constable, London.

de Margerie, E., Heim, A., 1888. Dislocations de L'écorce terrestre—Essai de définition et de nomenclature. Verlag von J. Wurster & Comp., Zürich.

Passchier, C.W., 2001. Flanking structures. Journal of Structural Geology 23, 951–962.

Playfire, J., 1802. Illustrations of the Huttonian Theory of the Earth. William Creech, Edinburgh.

Ramberg, H., 1963. Evolution of drag folds. Geological Magazine 100 (2), 97–106.

Srivastava, D.C., Lisle, R.J., 2004. Rapid analysis of fold shape using Bézier curves. Journal of Structural Geology 26, 1553–1559.

Suess, E., 1885. Das Antlitz der Erde. Tempsky, F.; Freytag, G., Prag and Wien; Leipzig.

Wiesmayr, G., Grasemann, B., 2005. Sense and non-sense of shear in flanking structures with layer-parallel shortening: implications for fault-related folds. Journal of Structural Geology, 27 (2), 249–264.